

## SEGMENTATION USING WAVELET AND GVF SNAKE

<sup>1</sup>Foon Dah Way, <sup>2</sup>Mandava Rajeswari, <sup>3</sup>Dhanesh Ramachandram  
School of Computer Science  
Universiti Sains Malaysia  
11800 Minden, Penang  
Malaysia  
(<sup>1</sup>dwfoon, <sup>2</sup>mandava, <sup>3</sup>dhaneshr)<sup>1</sup>@cs.usm.my

### ABSTRACT

The Gradient Vector Flow (GVF) snake is a popular technique to segment object in image processing. Its advantages are insensitivity to contour initialization and its ability to deform into highly concave part of the object compared to other deformable contour models. However, the performance of a GVF snake to model any arbitrary shape is heavily dependent upon objects with the highest intensity changes in the edge map and does not take into consideration objects with secondary gradient magnitude. To alleviate this problem, we propose a multi-scale method to obtain a suitable edge map to aid the GVF determination problem. The GVF are thus calculated from the enhanced edge map which focuses on the secondary structures of interest. This paper presents the approach and preliminary results which are encouraging.

### KEY WORDS

Gradient vector flow, wavelet, multi scale edge, and segmentation

### 1. Introduction

In computer vision, segmentation is a fundamental step prior to further processing and analysis operations performed on images. All segmentation approaches, regardless of the type of images they operate on, aim to segment an object of interest from the rest of the image structure. Image segmentation methods may be broadly divided into three categories: region based segmentation, contour based segmentation and morphological based segmentation approach [1]. This work presented in this paper focuses on the contour based segmentation.

The Gradient Vector Flow (GVF) snake [2] is a popular technique to segment object in image processing. Its advantages are insensitivity to contour initialization and its ability to deform into highly concave part of the object compared to other deformable contour models. However, the performance of a GVF snake to model any arbitrary shape is heavily dependent upon objects with the highest intensity changes in the edge map and does not take into consideration objects with secondary gradient magnitude. To alleviate this problem, we propose a multi-

scale method to obtain a suitable edge map to aid the GVF determination problem. The GVF are thus calculated from the enhanced edge map which focuses on the secondary structures of interest.

This is the extension work from our previous work on edge clustering using selected feature vector [3]. In that work, we propose an automated method to extract desired structures exclusively. The method focuses on automated scale selection and is based on wavelets. It utilizes wavelet edge detection, multi scale edge linking coupled with a method of classifying relevant edges. Several parameters from the scale evolution of the multi scale edges detected by a discrete wavelet decomposition of an image are used in a clustering algorithm to classify the edges belonging to background, structure(s) of interest, other structure(s) and noise. In this work, the preliminary initial boundary is used as the starting boundary in the well-established GVF snake [2]. The overall flow of the algorithm is illustrated in Figure 1:

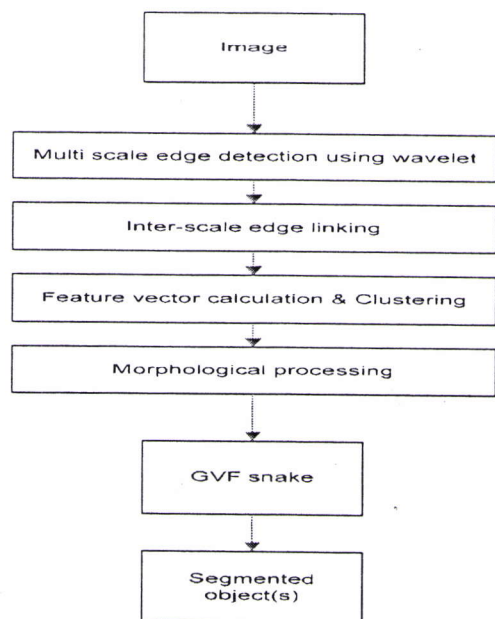


Figure 1: The overall of the flow of the segmentation algorithm.

## 1.1 GVF Snake

The popularity of the name *deformable models* or *snakes* is mostly credited to the work "Snakes" by Kass [4]. Deformable models are elastic manifolds (curves or surfaces) defined within an image domain that can move under influence of internal forces coming from within the manifold itself and external forces computed from the image data. A traditional deformable contour is a curve  $X(s) = [x(s), y(s)]$ ,  $s \in [0, 1]$ . If  $x(s)$  are the parameterized manifolds where  $s$  is the parameter of the manifold, the final contour determined by minimizes the representation of the energy of the manifold ( $E$ ) consist of internal energy ( $\mathcal{E}_{int}$ ) and external energy ( $\mathcal{E}_{ext}$ ) as follows:

$$E = \mathcal{E}_{int} + \mathcal{E}_{ext} \quad (1.1)$$

$$\mathcal{E}_{int} = \int_0^1 \frac{1}{2} (\alpha |X'(s)|^2 + \beta |X''(s)|^2) \quad (1.2)$$

where,

$\alpha$  is the weighting parameter control contour's tension

$\beta$  is the weighting parameter control contour's rigidity

$X'$  is the first derivative of  $X(s)$  with respect to  $u$

$X''$  is the second derivative of  $X(s)$  with respect to  $u$

$$\mathcal{E}_{ext} = E_{ext}(X(s)) ds \quad (1.3)$$

$E_{ext}$  is the external energy

It has been shown that the curve  $X(s)$  that minimizes  $E$  must satisfy the following Euler equation

$$\alpha X''(s) - \beta X''''(s) - \nabla E_{ext} = 0 \quad (1.4)$$

For a closed contour, we use a periodic boundary condition  $X(0) = X(1)$ . We can view Equation (2.4) as a force balance equation:

$$F_{int} + F_{ext} = 0 \quad (1.5)$$

where  $F_{int} = \alpha X''(s) - \beta X''''(s)$

$$F_{ext} = -\nabla E_{ext}$$

To find a solution for Equation (2.4), the deformable contour associates  $X$  with time  $t$  as in Equation 1.6:

$$X_t(s, t) = \alpha X''(s, t) - \beta X''''(s, t) - \nabla E_{ext} \quad (1.6)$$

In this method, the external force ( $F_{ext}$ ) is defined by a static force field call *gradient vector flow* (GVF) field  $F_{ext} = v(x, y)$ , yielding:

$$X_t(s, t) = \alpha X''(s, t) - \beta X''''(s, t) + v \quad (1.7)$$

Details for numerical solution to Equation (1.7) by discretizing the equation and solving the discrete system iteratively are found in [2]. The *edge map* is image feature that appears throughout the image spatial domain. The edge appears at places with high intensity contrast such as object boundaries. For the sake of completeness, we use edge map  $f(x, y)$

$$f(x, y) = -E_{ext}(x, y) \quad (1.8)$$

The gradient vector flow is the vector field  $v(x, y) = [u(x, y), v(x, y)]$  that minimizes the energy functional:

$$\mathcal{E} = \iint \mu (u_x^2 + u_y^2 + v_x^2 + v_y^2) + |\nabla f|^2 |v - \nabla f|^2 dx dy \quad (1.9)$$

The details of the numerical implementation of the GVF generation are found in [2]. The following section presents the methodology. Experiment is presented in Section 3. Discussion of the experimental results are reported in Section 4 and Section 5 is devoted to conclusion

## 2. Methodology

The wavelet coefficients of the image are obtained using a convolution wavelet transform algorithm in different scales, from fine to coarse [5] [6]. Edge detection is performed using wavelet transform modulus maxima to obtain multiple scale edges. Noisy edges are eliminated by maxima suppression with produces a collection of local maximum points. This process results in an edge map with edges representing highest intensity changes in the image. The next step is intra-scale linking with pruning to discard short edges. The estimation of the feature vector requires the chain of the maxima points traverse through different scales. An inter-scale edge linking method described in [3] is adopted. The feature vector used are edge strength (K), propagation number (N) and mean (M). The edge strength is chosen base on assumption that object boundary may have similar edge magnitude. Propagation number is chosen because it offers information on how far an edge may last from fine

to coarse detail. Mean is chosen as the third parameter because it measures the uniformity of the edge magnitude in multiple scales. These three parameters are used to cluster edges using a K-means clustering algorithm. The classification of the maxima chains based on edge strength, propagation number and mean may lead to classification of structures in the image. Then, two morphological processing steps are implemented consisting of dilation and thinning. Dilation aims to close the gap of the broken edges found in the desired edge map to form a continuous contour. Thinning is the process to make the contour shrink to 1 pixel in width, discarding the noise generated in the dilation process. These two processes are important to produce a closed contour as the output. Then, the desired edge maps are magnified by two times the edge strength in regions covered by the initial contour, whereas the edges in the other regions reduced by a factor of 0.5. This edge map is modified to give emphasis on the region of interest, which in this case, is the secondary structure object.

### 3. Experiment

The success of the proposed method in deforming the contour to the secondary structure in the image is verified through the experiment. The experiment results are shown in Figure 2 where (b) and (c) being the final contour overlaps on the image and final contour extracted using the original edge map. Figure 2(d) and (e) are the final contour overlaps on the image and final contour extracted using the enhanced and modified edge map which focuses on the small structure. The contour in 2(b) are deform toward the strongest edge magnitude, which is not the desired region, whereas contour in 2(d) deforms well to the desired region. The respective GVF field is shown in Figure 3(a) and (b).

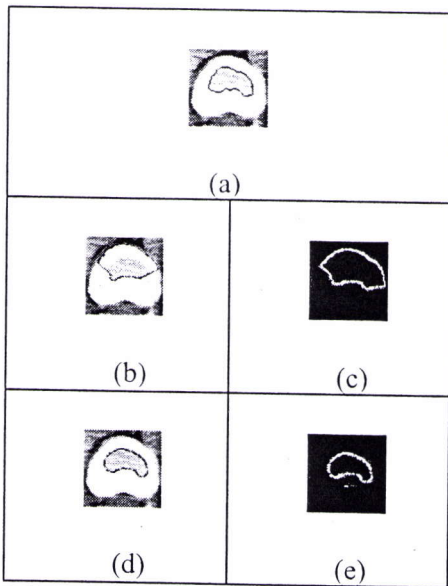


Figure 2: A CT image of a human abdomen region with initial contour display in grey colour. (b) The final

contour overlaps with the image after 100 iterations using original edge map. (c) The extracted final contour using the original edge map. (d) The final contour overlaps with the image after 100 iterations using modified edge map. (e) The extracted final contour using the modified edge map.

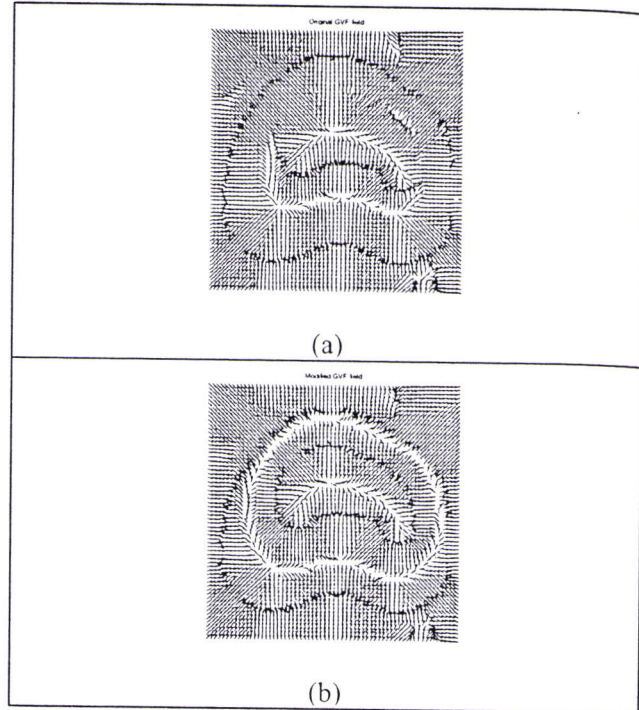


Figure 3: (a) The original GVF field which only attracts toward bigger object. (b) The modified GVF field attracts toward smaller object.

### 4. Discussion

The other segmentation results are shown in Appendix. The flexibility of the proposed method is elaborated in three main parts, that is: various cluster of edges, various object within a cluster, various object in different clusters.

The number of cluster is determined by the content of the image itself. For image in Figure 4, the number of cluster is equal to 3, whereas for image in Figure 5, the number of cluster is equal to 4. The number of clusters may be user-defined so that the best object outline/boundary is obtained. Figure 4(b), (c) and (d) are the edges of cluster 1, 2 and 3 respectively, while Figure 5(b), (c), (d) and (e) are the edges of cluster 1, 2, 3 and 4 respectively. The edges of interest are chosen manually or it can be obtained by image feature in an automatically manner. The chosen edge map is then processed with morphological operation which consists of dilation and thinning. Dilation is important to close gaps between broken edges to produce a continuous contour, and thinning is important to make the contour 1 pixel wide, discarding the artefact generated in the dilation process.

In the aspect of various objects within a cluster, this is shown in Figure 5(h) – (o), where the image in Figure

5(h), (i), (j), and (k) with white contour is the starting contour, and the image in Figure 5(l), (m), (n), and (o) with white contour is the fine contour after GVF snake deformation. In this example, there are 4 objects exist in the same cluster of edges, and the proposed method successfully retrieves all objects.

For some objects, they are clustered into different cluster of edges because of their difference of edge strength and ability to survive against different scale. For this type of image, the proposed method shows good performance in detecting the objects. For Figure 6(b) and (c) are the starting contour for 2 different objects exists in 2 different clusters of edges, and the Figure 6(f) and (g) shows their final contour after GVF snake each.

The rest of Figure 6 is some of the other results obtained for different image. For a special case of Figure 6(a) and (e), this particular object are obtained by using the second highest center of cluster value in the feature space, to detect the round shape object in the center, instead of the high intensity stripe. This shows the method can be adjusted and adapted to detect small structure in an image in our previous work [2].

## 5. Conclusion

We have introduces a new concept in image segmentation where the aim is to extract objects closed contour from the image. Firstly, the obtained closed contours are useful to modify the edge map where the secondary structures are the place to focus on. We have shown that computation of the GVF field using the modified edge map that allows for contour initialization into the secondary structure and enables convergence to its boundary. Secondly, the proposed method also showed capability to detect multiple objects in an image. This is particular of interest in object detection and recognition. Thirdly, with the concept of clustering of edges is

equivalent to classify objects in the image, the proposed method are capable to label different class of objects detected. This concept is important to semantically labelling of the image for analysis and retrieval purposes.

## Acknowledgements

The authors would like to thank The Ministry of Education, Malaysia for funding this research, through FRGS grant 304/PKOMP/670027.

## References:

- [1] M. Sonka, V. Hlavac & R. Boyle, *Image processing, analysis and machine vision* (Cambridge: International Thomson Computer Press, 1996)
- [2] C. Xu, & J. L. Prince, Snakes, shapes, and gradient vector flow, *IEEE Transaction on Image Processing*, 7(3), 1998, 359-369.
- [3] D.W. Foon, M. Rajeswari & D. Ramachandram, Automated extraction of small structures in medical images based on multi scale approach. *Proc. Int. Conf. on Cybernetics and Information Technologies, Systems and Application*, Florida, USA, 2004, 81-84.
- [4] M. Kass, A. Witkin, & D. Terzopoulos, Snakes: active contour models. *International Journal of Computer Vision*, 18(4), 1987, 321-331.
- [5] S. Mallat, & Z. Zhong, Characterization of signals from multiscale edges, *IEEE Transaction on Pattern Analysis and Machine Intelligence*, 14(7), 1993, 710-732.
- [6] S. Mallat, *A wavelet tour of signal processing* (Academic Press, UK, 1966).

## Appendix

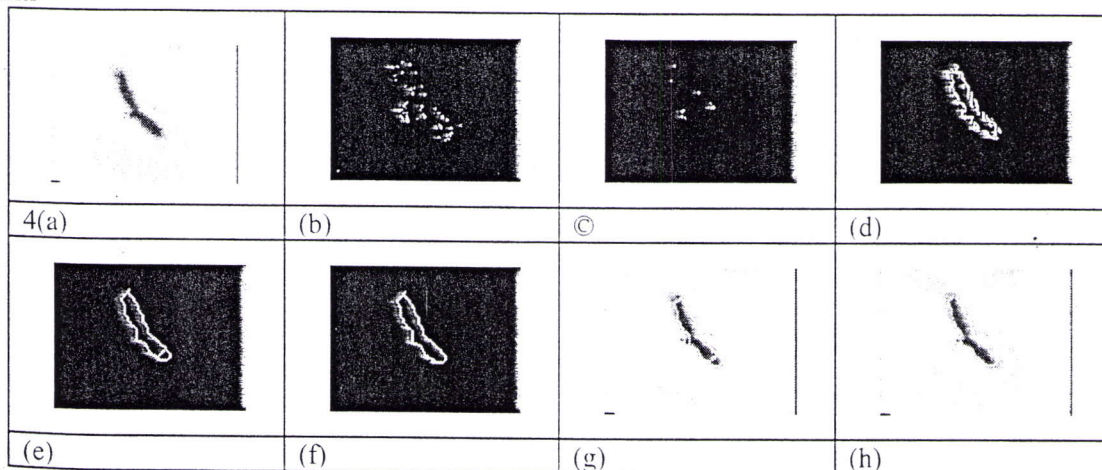


Figure 4: (a) The original image. (b) (c) (d) The edge map of cluster 1, 2 and 3 respectively. (e) The edge cluster 3 after dilation and thinning. (f) The edge cluster 3 after short edge reduction. (g) (h) The overlap starting contour to the original image and the final contour overlap to the original image respectively.

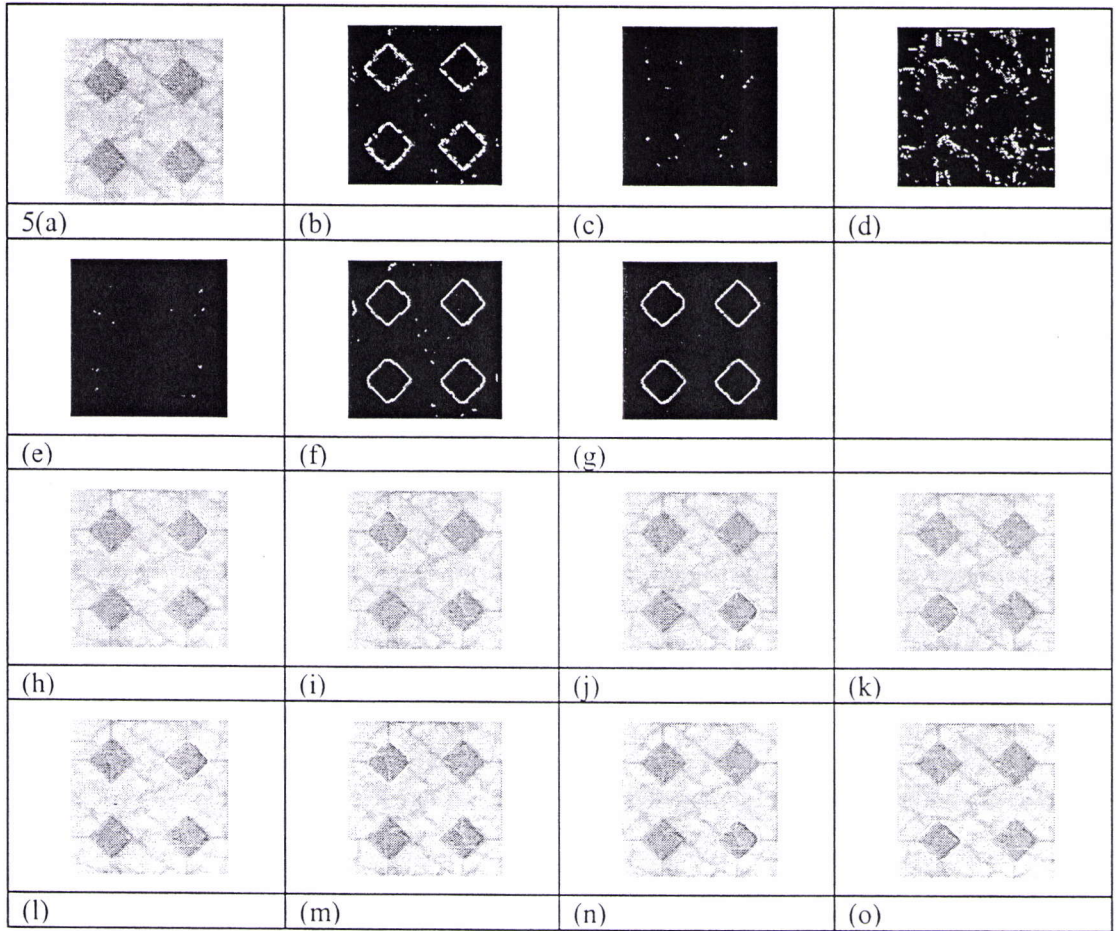


Figure 5: (a) The original image. (b) (c) (d) (e) The edge map of cluster 1, 2, 3 and 4 respectively. (f) The edge cluster 1 after dilation and thinning. (g) The edge cluster 1 after short edge reduction. (h) (i) (j) (k) The overlap starting contour to the original image for different objects. (l) (m) (n) (o) The final contour overlap to the original image respectively for different objects.

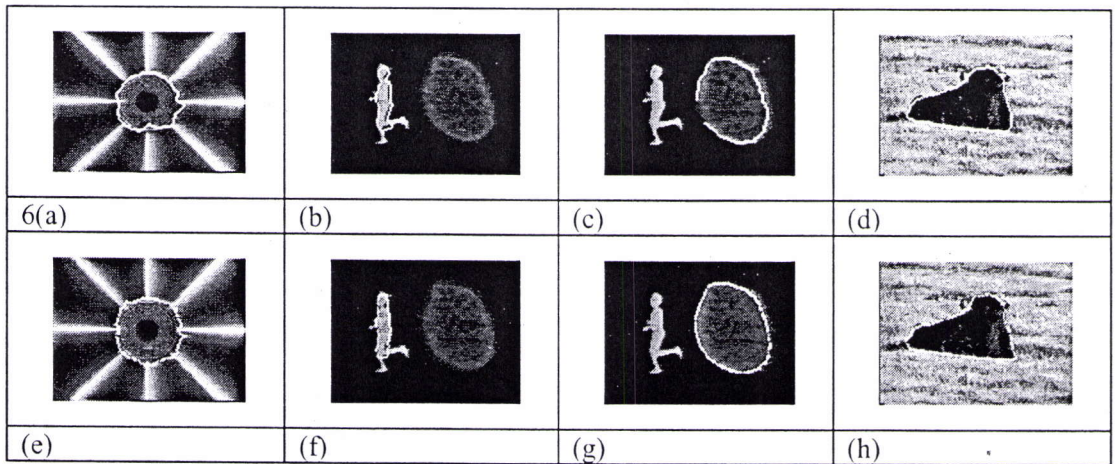


Figure 6: (a) (b) (c) (d) The overlap starting contour to the original image of different objects. (e) (f) (g) (h) Their respective final contour overlaps to the original image for different objects.